

# Studying focal ratio degradation of optical fibres with a core size of 50 $\mu\text{m}$ for astronomy

A. C. Oliveira,<sup>1\*</sup> L. S. de Oliveira<sup>1\*</sup> and J. B. dos Santos<sup>2\*</sup>

<sup>1</sup>Laboratório Nacional de Astrofísica, Rua Estados Unidos 154, Bairro das Nações, CEP 37.500.000, Itajubá, MG, Brazil

<sup>2</sup>Instituto de Física de São Carlos/USP, Av. Trabalhador São Carlense 400, Caixa Postal 369, CEP 13.560-970, São Carlos, SP, Brazil

Accepted 2004 October 20. Received 2004 October 19; in original form 2004 February 3

## ABSTRACT

Along with the spectral attenuation properties, the focal ratio degradation (FRD) properties of optical fibres are the most important for instrumental applications in astronomy. We present a special study about the FRD of optical fibres with a core size of 50  $\mu\text{m}$  to evaluate the effects of stress when mounting the fibre. Optical fibres like this were used to construct the Eucalyptus integral field unit. This fibre is very susceptible to the FRD effects, especially after the removal of the acrylate buffer. This operation is sometimes necessary to allow close packing of the fibres at the input to the spectrograph. Without the acrylate buffer, the protection of the cladding and core of the fibre may be easily damaged. In the near future, fibres of this size will be used to build the Southern Observatory for Astronomical Research (SOAR) integral field unit spectrograph (SIFS) and other instruments. It is important to understand the correct procedure which minimizes any increase in FRD during the construction of the instrument.

**Key words:** instrumentation: miscellaneous – instrumentation: spectrographs.

## 1 INTRODUCTION

Mode-dependent loss mechanisms are the causes of focal ratio degradation (FRD) in optical fibres, and are not often addressed by manufacturers. Mode-dependent losses can be divided into two basic mechanisms. The first is waveguide scattering, which causes transfer of energy into lossy modes by variations of the core diameter along the length of the fibre. The second is mechanical deformation. Mechanical deformation is a change of the geometry of the fibre away from a straight cylinder. Large-scale bending, or macrobending, is where the radius of curvature of the bend is very large in comparison to the core diameter. On the other hand, microbends are deformations of the cylindrical core shape which are small compared to the fibre diameter (Ramsey 1988). It is well known that mechanical deformation causes FRD by the formation of microbends in the fibre (Clayton 1989). FRD is a non-conservation of *étendue* (or optical entropy) such that the focal ratio is broadened by propagation in the fibre. When mounting the fibre, the appropriate epoxy and tubing should be selected, and general care must be taken to minimize mechanical stress and avoid additional FRD.

FRD may be a source of scattered light in spectrographs fed by optical fibres from an integral field unit (IFU). The GMOS IFU has 1500 fibres with a core size of 67  $\mu\text{m}$  and uses an output lenslet to minimize the throughput loss due to focal degradation (Murray et al. 2002). The situation is worst when it is necessary to remove the

acrylate buffer of the fibres. Sometimes this operation is necessary to build a linear slit with a reduced centre-to-centre distance for the fibres, such as the SPIRAL (Kenworthy, Parry & Taylor 2001) and Eucalyptus (Cesar et al. 2002) IFUs. The removal of the acrylate buffer reduces the protection to the cladding and the core, so that the optical fibre may be exposed to high stress. During optical tests of the Eucalyptus IFU, the slitlet blocks were identified as a source of FRD. This may be a result of the close packing of the fibres on the slitlet resulting in mechanical stress.

## 2 MEASUREMENT OF FOCAL RATIO DEGRADATION

Astronomers recognized early the necessity of performing measurements of FRD. The published literature is quite informative in this regard (Angel et al. 1977; Barden et al. 1980, 1981; Gray 1983; Lund & Enard 1983; Powell 1983; Ramsey & Huenemoerder 1986). Measurements of the FRD are reasonably straightforward. The methods used by Powell (1983) and others (Lund & Enard 1983; Guerin & Felenbok 1988) are a clear improvement on the early technique employed by Angel et al. (1977) and Barden et al. (1981). Most of the FRD measurements to date are relative in nature; that is, they assume that all light is transmitted at some lower limit of the output *f*-ratio. The measurements of Powell (1983) are an exception to this as they are absolute. While relative measurements are quite adequate for many purposes, they can be misleading when assessing the fibre performance at relatively fast *f*-ratios ( $f/\# < 3.0$ ) or looking at small core fibres. An apparatus that measures the amount

\*E-mail: cesar@lna.br (ACO); ligia@lna.br (LSdO); cacau@if.sc.usp.br (JBdS)

of light output from the fibre relative to that input with a given mode distribution is described by Ramsey (1988). The scheme, originally designed by Barden while he was at Penn State, compares the light in the input beam to that emanating from the fibre by way of a simple  $90^\circ$  flip of two separate mirrors.

In this work we have used the same method used by Lee, Haynes & Skeen (2001) and originally developed by Carrasco & Parry (1994). This method does not use mirrors to provide a reference and produces relative measurements. This type of result can be used for comparative analyses and is sufficient for a study of the effects of stress on the optical fibres.

### 3 SUMMARY OF FIBRE ISSUES

#### 3.1 Types of fibre tested

The optical fibre tested was the same used to build the Eucalyptus IFU; it was made by Polymicro Technologies. Specifications for this fibre, FVPA0500600700200, are given in Table 1.

This fibre is very susceptible to the effects of FRD. The main reason is the ratio of the diameters of the inner polyimide buffer and the core, coupled with the small physical size. This ratio is very small so that the protection of the core by the polyimide buffer is not enough to support a large stress when the acrylate buffer is removed. High  $\text{OH}^-$  silica fibre was selected to provide the best transmission in the blue. The spectral attenuation is shown in Fig. 1. We need at least  $5\text{-}\mu\text{m}$  cladding thickness to avoid light loss at the longest wavelength ( $1\ \mu\text{m}$ ). The blue fibre exhibits a deep absorption at about  $950\ \text{nm}$ . Because it coincides with an atmospheric absorption, it is not a region of interest for observations.

#### 3.2 Mounting of the fibres

The optical fibres are generally mounted in some form of connector and sometimes in special structures. The Eucalyptus IFU has two

**Table 1.** Specification of the Eucalyptus IFU fibre.

Type of fibre	High $\text{OH}^-$
Length	2 m
Numerical aperture	$0.22 \pm 0.02$
Core	$50\ \mu\text{m}$
Cladding	$60\ \mu\text{m}$
Inner buffer (polyimide)	$70\ \mu\text{m}$
Outer buffer (acrylate)	$200\ \mu\text{m}$

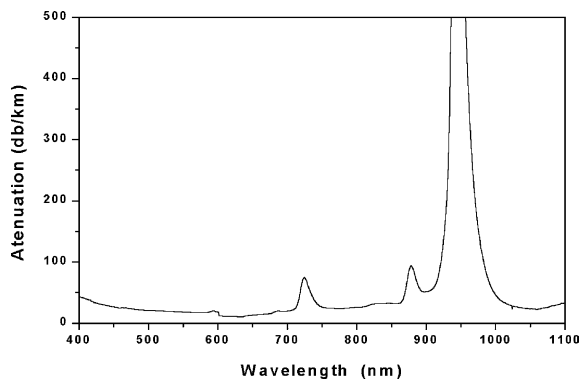


**Figure 1.** Spectral attenuation curve for blue fibre between 350 and 1000 nm.

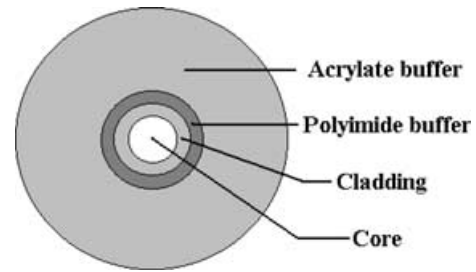


**Figure 2.** Schematic diagram of the optical fibre.

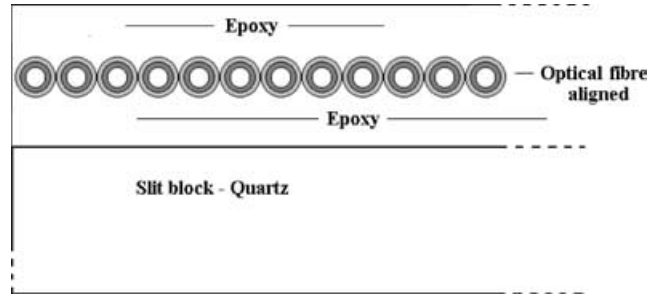


**Figure 3.** Schematic diagram of the slit block with the optical fibres aligned.

types of termination: input microhole arrays and output slit blocks. We are especially interested in evaluating the construction of the slit blocks. During optical tests of the Eucalyptus IFU, the slit blocks were identified to be a source of FRD. This may be a result of the close packing of fibres on the slit block and the utilization of the Araldite epoxy, resulting in mechanical stress. A dual buffered fibre (Fig. 2) was chosen for a number of reasons. However, to allow closer packing of the fibres at the output slit, the outer acrylate buffer can be readily removed so that the fibres can be assembled with a spacing determined by the inner polyamide buffer, as shown in Fig. 3.

The blocks for the Eucalyptus slit were made with brass. However the block tests were made with quartz to avoid the problems of differential thermal expansion. The analysis of Fig. 3 shows that there is no contact between the line of the fibres and the top of the quartz block. This gap is necessary to avoid injuries on the polyimide buffer by the base of the quartz. In order to perform the tests, two fibre bundles were prepared, each with 40 fibres and each 2 m long.

For easy handling, all fibres of the experimental input array, were mounted in a typical ferrule connector, as shown in Fig. 4. The fibre was first placed within a flexible tube (polyamide or similar), often referred to as the strain relief tube. The fibre and tube were then placed within a rigid ferrule (usually made of stainless steel). The role of the strain relief tube is to prevent stress occurring at the point where the fibre enters the ferrule, as this may lead to breakages. Adhesive was applied to the fibre and tubing to cement it in place. The ferrule can be easily manipulated for polishing and mounting in an experiment to measure the FRD, without risk of damaging the delicate fibre.

#### 3.3 Types of adhesive tested

The adhesives selected must have cure times of the order of 24 h and low shrinkage whilst curing. Long cure times are desirable to provide plenty of time to assemble parts without the glue becoming unworkable. In general, longer cure times also imply lower glue stresses during the curing process. It is important to use epoxies

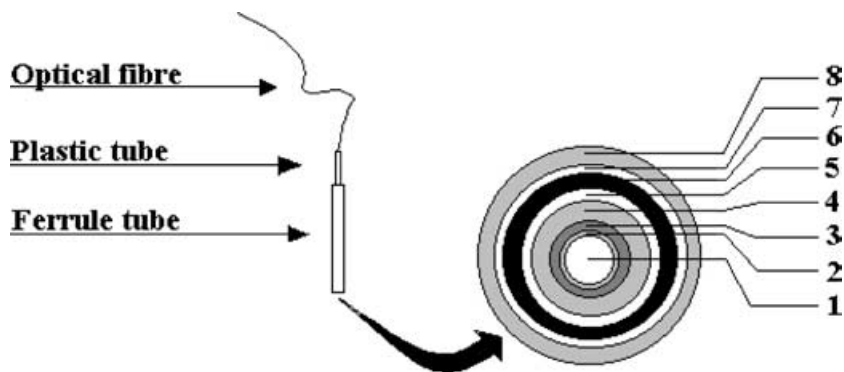


**Figure 4.** Schematic diagram of a single fibre mounting assembly: 1, core; 2, cladding; 3, polyimide buffer; 4, acrylate buffer; 5, epoxy; 6, plastic tube; 7, epoxy; 8, ferrule tube.

with low shrinkage to avoid stress being exerted on the fibre as the glue cures. The slit blocks of the SPIRAL and Eucalyptus IFUs were made using Araldite K106. The reason for this choice was the mechanical difficulty of keeping an epoxy like EPOTEK around the block. This epoxy has low viscosity and runs down to the edge of the clamps. However, optical tests show that the main source of FRD in the systems comes from the slit blocks. To know if such a problem was caused by the glue itself, we prepared test fibres using two types of adhesives, EPOTEK 301-2 and Araldite K106. The idea was to make two blocks under the same conditions: same fibres, same length of fibres but with different epoxies. To make a slit block using EPOTEK, it was necessary to develop special apparatus with adequate design (Figs 5 and 6).

During the cure of the epoxy, it was necessary to hold the polytetrafluoroethylene (PTFE) blocks in the correct position by using a clamp with screws (Fig. 7). The material of the clamp was aluminium and the base of the metal was machined at an angle. This angle is necessary to obtain a slope on the level of the epoxy. This is important, in order to obtain more area to polish on the polishing plane and to avoid damage during the procedure.

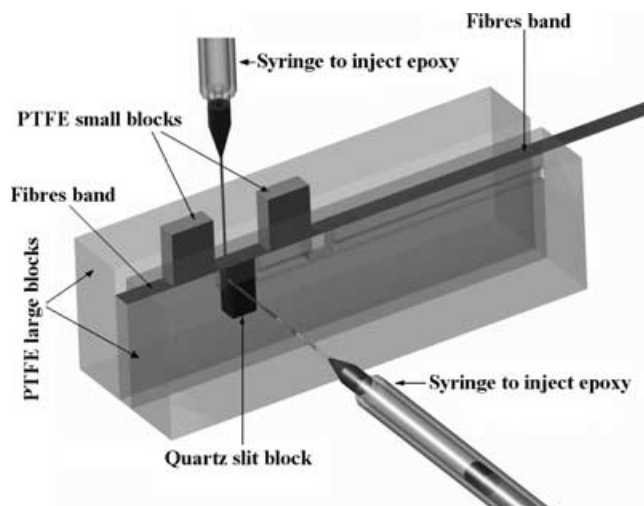


**Figure 5.** Diagram of the apparatus to hold the fibres in position on the slit block. The system consists of PTFE blocks that are joined with silicone glue to avoid loss of the EPOTEK epoxy before the cure. The quartz slit block is inserted between the PTFE blocks under the fibre band. The epoxy is then injected by syringes shown in the figure. PTFE is easy to machine and does not adhere to the parts. This condition is very important for removal of the parts of the block system after the epoxy has cured.

### 3.4 Fibre preparation

All optical fibres were carefully prepared in the polishing laboratory at the Laboratório Nacional de Astrofísica (LNA). First, the slit blocks were mounted and the other ends of the fibres were mounted into the tubes. The fibre and tubing were glued into a ferrule and allowed to cure. After curing, the glue was removed prior to polishing. To obtain the maximum throughput, the surfaces of the fibres should be polished such that they are optically flat and free from scratches. The polishing process consists of roughing off with 2000-grit emery paper and polishing using 6- $\mu\text{m}$  diamond slurry on a copper plate, then 1- $\mu\text{m}$  diamond slurry on a lead/tin plate, and finally colloidal silica solution on a chemical cloth. All polishing was carried out on a lapping machine using polishing jigs developed at LNA. The same conditions were used to polish both slit blocks.

## 4 EXPERIMENTAL PROCEDURE

Basically, to measure the FRD properties of a fibre it is necessary to illuminate the test fibre with an input beam of known focal ratio. Then, the output beam can be measured to determine the amount of FRD produced by the test fibre. The experimental apparatus used to achieve this is illustrated in Fig. 8.

Illumination was provided via a fibre-optic light source with a stabilized quartz-halogen lamp. The source fibre (2 m, 100  $\mu\text{m}$  core) was mode scrambled to provide uniform illumination. The output of the source fibre is collimated using an achromatic collimator lens (focal length = 200 mm). A bandpass filter was used to provide light of known wavelength. The collimated beam was then coupled into the test fibre with a commercial camera lens (focal length = 40 mm). An iris diaphragm placed in the collimated beam can be used to select the input focal ratio. An alignment CCD, fed by a beamsplitter, allows the image of the source fibre to be accurately positioned with respect to the test fibre by means of observation on a television monitor. To ensure accurate alignment of the fibre with the optical axis of the camera, the fibre was mounted in a tip-tilt translation stage. Finally, the output of test fibre was re-imaged on to a CCD camera. To begin the experiment, the image of the test fibre was brought into focus on the CCD. A defocus of  $8 \pm 0.01$  mm was then applied to the CCD so that it was illuminated with a cone of light from the test fibre. Images like that presented in Fig. 9 show the output cone from a test fibre and can then be examined over a range of focal ratios. Background exposures were also taken for subtraction from the test exposures to remove the effects of hot pixels, stray light, etc. The images were analysed using the IRAF routines QPHOT and PPOFILE (Tody 1993).

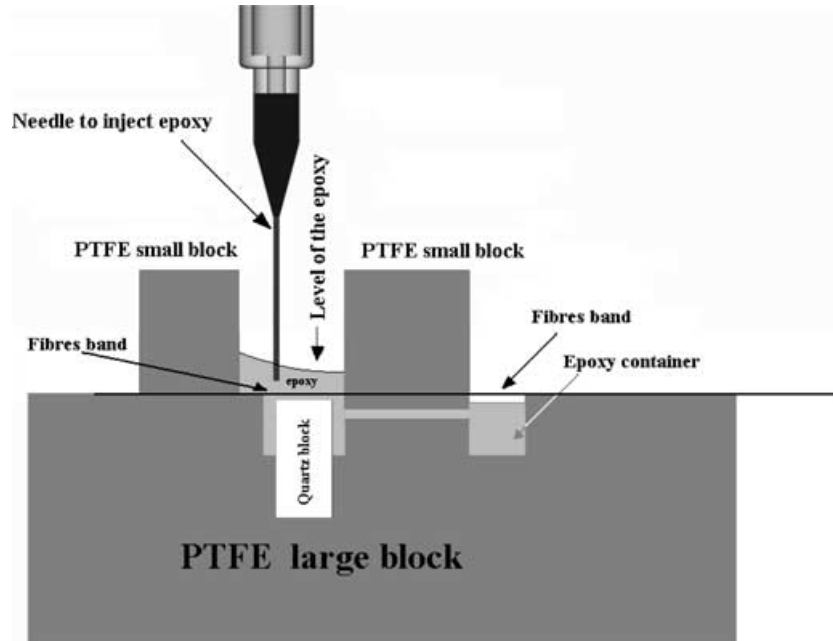


**Figure 6.** Schematic diagram of the PTFE blocks to manufacture the slit block. A multiblock system was chosen to make it easy to remove the components after the glue has cured. The best material for the components of the system is PTFE doped with graphite.

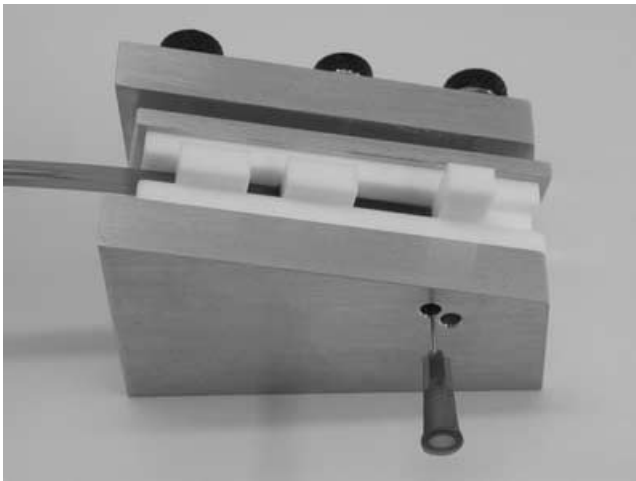


**Figure 7.** Photograph of the clamp to hold the apparatus to manufacture the slit blocks.

Aperture photometry was performed on the image to determine the flux within a known focal ratio relative to the flux present within an  $f/2$  cone. The limiting focal ratio that can propagate in the fibres tested was approximately  $f/2.2$ . The  $f/2$  re-imaging optics will therefore collect all of the light from the test fibre. The fibres were tested at a wavelength of  $525 \pm 50$  nm (defined using a Schott glass VG14 colour filter). Tests were not carried out at infrared wavelengths because a suitable infrared detector system was not available. Although FRD is known to increase with wavelength (Carrasco & Parry 1994), the effect is small. The performance in the infrared can therefore be expected to be very similar to that measured in the optical. Any change in FRD with wavelength is likely to be dominated by diffraction.

## 5 SUMMARY OF RESULTS

### 5.1 Optical analysis

Microscope photographs of two slit blocks were obtained after the final polishing and can be seen in Figs 10 and 11. The analysis shows that the fibres do not keep the alignment after the cure of the Araldite epoxy. On the other hand, the fibres keep the alignment after the cure of the Epotek epoxy. It was verified that the alignment before introducing the epoxy was perfect for both slit blocks. However, the viscosity of Araldite is not the same as Epotek 301-2, causing the fibres to displace during its injection. Still, Fig. 10 shows that Araldite curing is not homogeneous. One can note several bubbles that may be responsible for some stress on the fibres.

It is possible to see many micropores in the Araldite block, but few in the Epotek block. There are no micropores on the quartz face so that the quality of the polishing is the same on both slit blocks. This difference is not dependent on the polishing time. Several tests were performed by applying consecutive increments of time during the polishing process. The micropores are the microbubbles visible after the polishing and they appear in the whole volume of the Araldite epoxy.

The fibre end quality was visually inspected at all stages during the polishing process to ensure high performance. The optical flatness of the fibres was also confirmed by testing with a microscope interferometer. An optical test was made with a flat field set at the input of the fibres. In this test, the fibre input ends were illuminated with a collimated beam and the image of the fibre output, at the block, was taken with a CCD detector fastened at an inverted microscope. The assessment procedure consisted of the analysis of the cross-section of the fibres aligned in the slit block (Figs 12 and 13).

The structure seen in the image is a combination of the light from the microscope reflected by the slit block surface and the light from the fibre cores. For this reason, it is possible to see the polyimide buffer illuminated by the microscope light. The results at the bottom

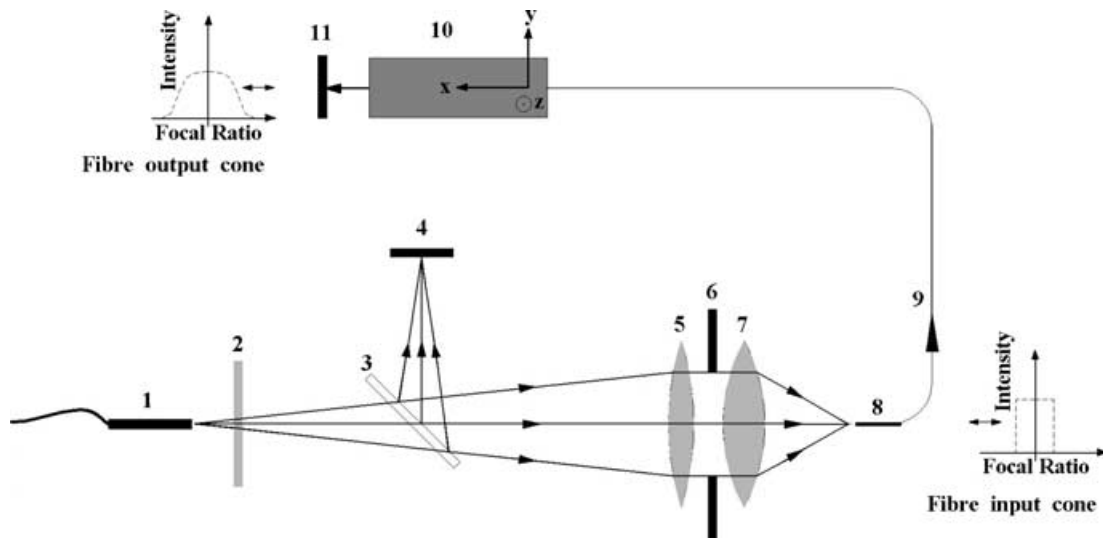


**Figure 8.** Diagram of the apparatus used to measure FRD: 1, source fibre (mode scrambled); 2, filter; 3, beamsplitter; 4, alignment CCD; 5, collimator lens; 6, adjustable iris diaphragm; 7, camera lens; 8, ferrule of the test fibre; 9, test fibre; 10, slit block; 11, CCD detector with re-imaging lens. The slit block on test is placed on an  $x y z$  translation stage to obtain the correct position with respect to the centre of the CCD.

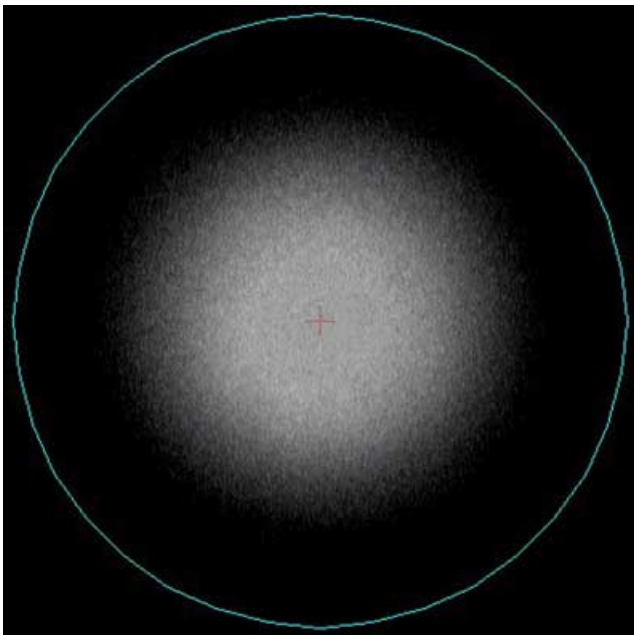


**Figure 9.** Image of an FRD cone, measured with an  $f/5.5$  input beam from the test fibre. The size of the circumference is  $f/2$ .

of the figures are obtained using the integrated flux within the range of the image. The analysis shows that the Epotek slit block has a more uniform distribution of light than the Araldite slit block and this test confirms the optical quality of the polishing of the fibres in the slit block.

## 5.2 Focal ratio degradation analysis

Plots of enclosed energy versus output focal ratio are shown in Figs 14 and 15. All 40 fibres of each block were tested, but we have plotted just the extreme curves. The other curves are positioned between the best curve and the worst curve. The focal ratio output of  $f/5.5$  was taken for comparison. It is important to test fibres at

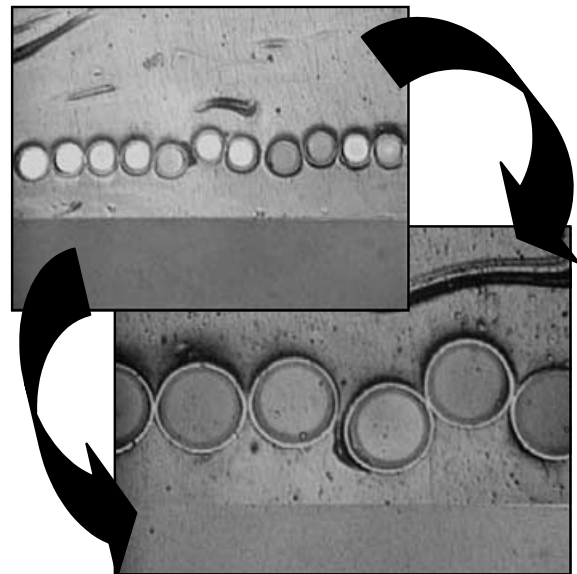


**Figure 10.** Microscope images of part of the slit block constructed with Araldite K106 epoxy, after the final polishing.

a focal ratio of approximately  $f/5$  as this is generally accepted as the optimum focal ratio for use with fibres. Slower beams are inefficient as a result of increased FRD losses, while faster beams require expensive collimator optics in the spectrograph and the image scrambling properties of the fibres are typically worse (Ramsey 1988). The Araldite slit block has fibres with enclosed energy, at  $f/5.5$ , between 52 and 90 per cent. The Epotek slit block has fibres with enclosed energy between 75 and 90 per cent at the same focal ratio. The range of light lost in the Araldite slit block is larger than in the Epotek slit block.

### 5.2.1 Tests of fibres in ferrules

Several tests were made in samples consisting of 50- $\mu\text{m}$  core fibre, 2 m long, both extremities mounted in a typical ferrule connector

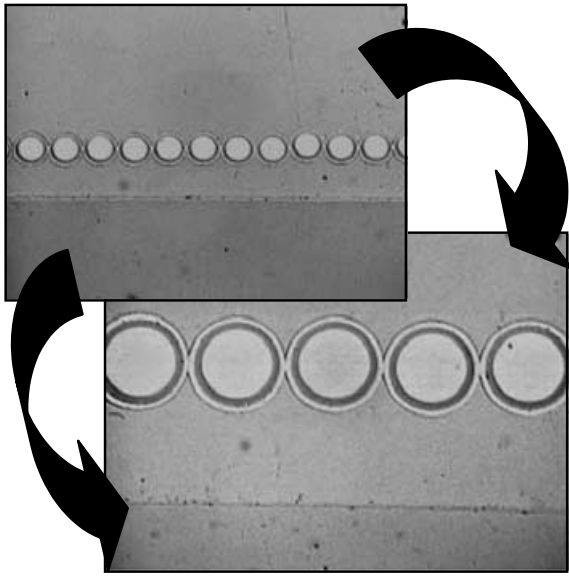


**Figure 11.** Microscope images of part of the slit block constructed with Epotek 301-2 epoxy, after the final polishing.

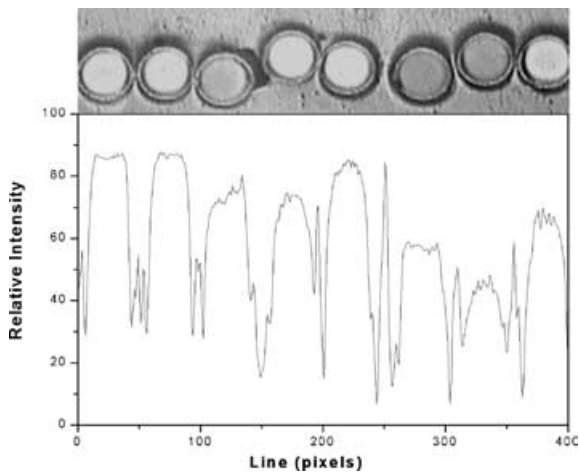


**Figure 12.** Top: partial photograph of the Araldite slit block showing the individually resolved images of each element. The dispersion direction is vertical. Bottom: cross-section in the spatial direction.

(Fig. 4). The objective was to evaluate the FRD performance of these samples and to compare with the fibres mounted on the slit block. In these connectors, the choice of glue does not change the FRD performance of the fibres because the outer acrylate buffer is not removed. In fact, there was no difference in the FRD performance between the fibres mounted with Epotek or with Araldite. However, for easier manipulation, it is advisable to use quite viscous adhesive (Araldite). The results presented in Fig. 16, obtained from the  $f/5.5$  input beam, show the best and the worst curves obtained after measuring the performance of the 40 test fibres. The enclosed energy curve shows that the energy contained within an  $f/5.5$  aperture lies between 83 and 90 per cent. The accuracy of these results is  $\sim \pm 1$  per cent, although FRD properties may vary slightly for different fibres as a result of the difficulty of assembling each fibre in exactly the same manner. These results may represent the geometric throughput of the fibre under test so that it is interesting to compare with the results shown (Fig. 14). The comparison

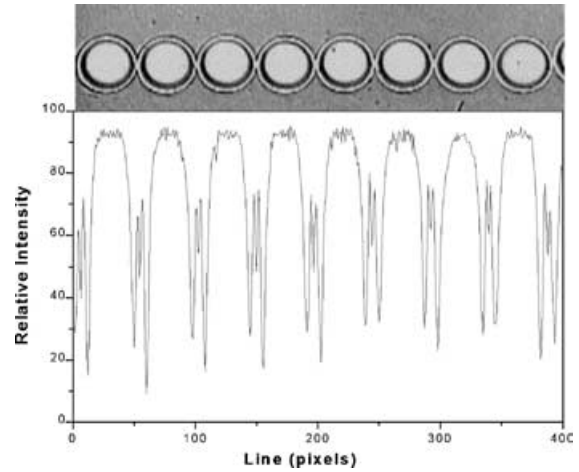


**Figure 13.** Top: partial photograph of Epotek slit block showing the individually resolved images of each element. The dispersion direction is vertical. Bottom: cross-section in the spatial direction.

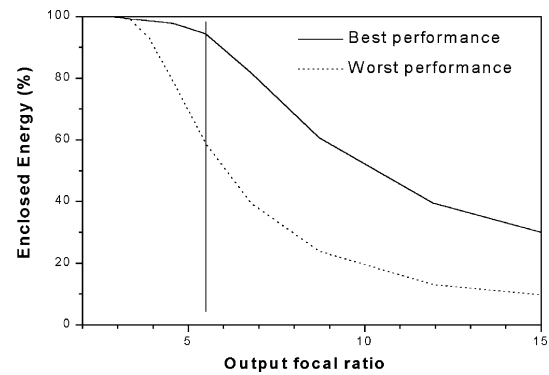


**Figure 14.** Plot of enclosed energy versus focal ratio for the Araldite slit block fibres. The FRD performance of all fibres is defined by curves located between the best and worst cases. The solid vertical line indicates the input focal ratio of  $f/5.5$ .

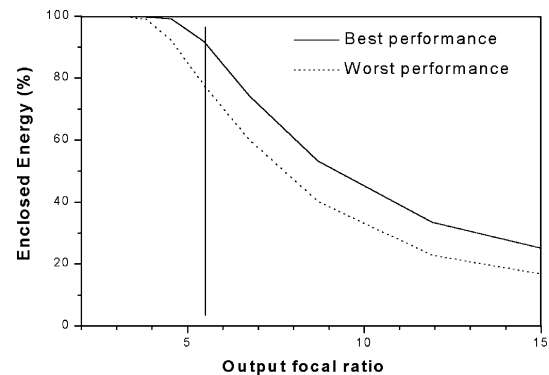


**Figure 15.** Plot of enclosed energy versus focal ratio for the Epotek slit block fibres. The FRD performance of all fibres is defined by curves located between the best and worst cases. The solid vertical line indicates the input focal ratio of  $f/5.5$ .

shows similar results between the curves, and the conclusion is that it is possible to optimize the FRD performance of the fibres on the slit block using Epotek instead Araldite. In other words, the FRD performance of the Epotek slit block fibre was as good as the FRD performance of the fibre with ferrules at both ends. The steel ferrule

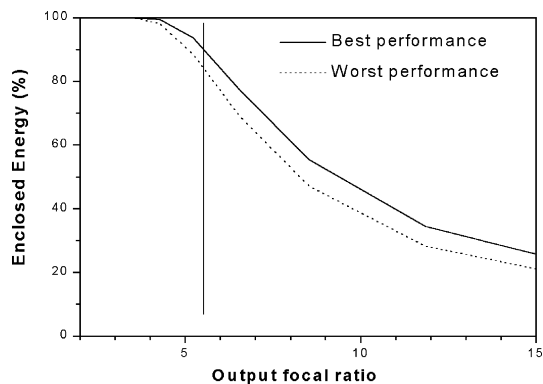


**Figure 16.** Plot of enclosed energy versus focal ratio for the test fibres with steel ferrule, polyimide tube and Araldite adhesive in both extremities.

at the end of the fibre, mounted with Araldite or Epotek, is not a source of the FRD at room temperature. However, the results of Lee et al. (2001) clearly demonstrate that steel ferrules cannot be used at cryogenic temperatures because of the increase in FRD. In this case, the increased FRD is thought to be caused by contraction of the metal ferrule at low temperature causing stress on the fibre.

### 5.2.2 Histogram analyses

The distribution of throughputs as measured within an  $f/5.5$  cone are plotted as histograms for each slit block (Figs 17 and 18) and for the case of fibres in ferrules (Fig. 19).

The analyses of Figs 18 and 19 strongly suggest a random scatter in throughput about a mean value with a normal curve centred around 87 per cent, for the Epotek slit blocks and the fibres in ferrules. In these cases, it is reasonable to presume that there is a spectrum of stress levels associated with imperfections in the core/clad boundary that deviate the shape of the fibre from that of a perfect cylindrical waveguide. These microbends cause the light to be scattered into a larger numerical aperture (NA). On the other hand, the histogram of Fig. 17 may be divided into two distributions. The cluster of high values is similar to those in Figs 18 and 19, while the lower value cluster of measures represents an additional component to the FRD. It may therefore be supposed that there are two different

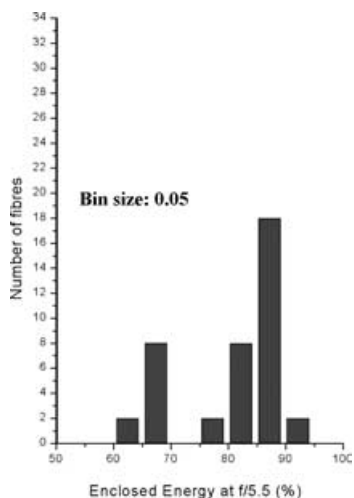


**Figure 17.** Araldite slit block histogram plot of the enclosed energy measured at  $f/5.5$ , in 40 fibres.

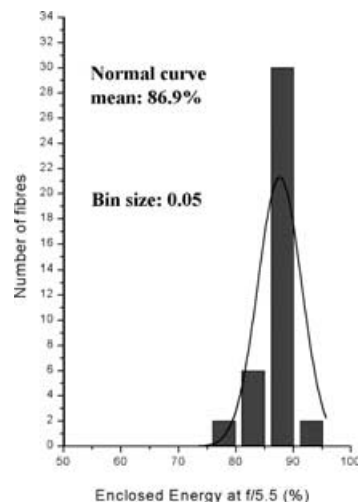


**Figure 18.** Epotek slit block histogram plot of the enclosed energy measured at  $f/5.5$ , in 40 fibres.

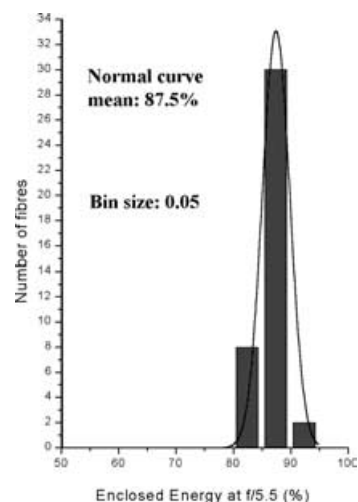


**Figure 19.** Fibres in ferrules histogram plot of the enclosed energy measured at  $f/5.5$ , in 40 fibres.

contributions to the FRD in the slit block constructed with Araldite. The first contribution, similar to the Epotek slit block and the fibres in ferrules, is probably caused by the microbending process. The second contribution may provide evidence for stresses caused by the epoxy. In fact, microscope inspection reveals that, after drying, the Araldite epoxy is not homogeneous and this difference may induce the formation of local areas of stress.

### 5.3 Tests with different lengths of blocks

The width of the slit block can be defined just by the number of fibres that form the linear array. After removing the outer acrylate buffer, the fibres were assembled with a spacing determined by the inner polyimide buffer (see Table 1). Therefore, to make a slit block with 40 fibres it was necessary to use a quartz block with a width of 2.8 mm. The length and the height of the block were a free choice but an increase of length on the slit block means an increase of area of contact with epoxy on the fibres. The result may be an increase of the mechanical stress at the ends of the fibres. To evaluate the effects of length of the slit block, we have tested this with several

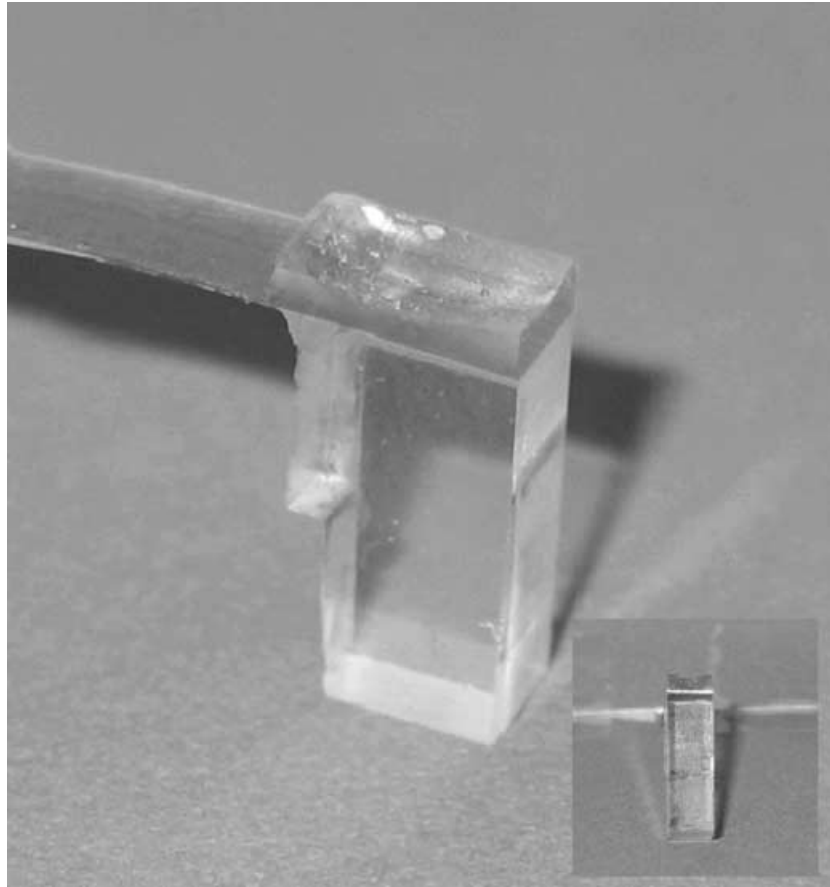


**Figure 20.** Photograph of a quartz slit block 5 mm in length. The front of the block, 2.8 mm in width, with the band fibres illuminated is shown on the right.

blocks with different lengths. There was no significant difference with blocks smaller than 10 mm. However, it is very difficult to avoid high stress at the fibre band on blocks larger than 10 mm in length. This may be a result of the difficulty of keeping a band of fibres aligned at a length larger than 10 mm without mechanical stress. The best choice for supporting the fibres was a block with a length of 5 mm (Fig. 20).

## 6 SUMMARY AND CONCLUSIONS

We present here the design, construction, FRD tests and results obtained for fibres with a core size of 50  $\mu\text{m}$  supported on slit blocks of quartz. To construct the slit blocks for an IFU, it is necessary to remove the acrylate buffer of the optical fibres. This procedure is required to obtain close packing of fibres at the slit to the spectrograph. However, small core fibres (50  $\mu\text{m}$ ) are very susceptible to increased FRD effects, especially after the removal of the acrylate buffer. The motivation of the work presented in this paper was to improve the performance obtained in the construction of the slit blocks used in SPIRAL and Eucalyptus IFUs. In both instruments, we have a decrease of throughput caused by high FRD in the slit blocks. In this work we have used smaller blocks than were used in SPIRAL and Eucalyptus IFUs. The idea was to reduce the length of the fibres inside the epoxy to reduce the stress area at the end of the fibres. However, the most important analysis was made on the type of epoxy used to build the slit blocks. Two different epoxies, Araldite k106 and EPOTEK 301-2, were used to construct two slit block with 40 fibres, 2 m long. It was shown that the EPOTEK epoxy is better

than the Araldite epoxy to build the slit blocks. Results of FRD tests show that the EPOTEK block is more stable and the FRD curves have a smaller range. The microscope images show that Araldite is not homogeneous after the cure and the result is several stress points around the fibres. The consequence is displacement of the fibres and poor FRD performance. The cross-section of a flat-field image shows that the EPOTEK block has a distribution of light that is more homogeneous than that of the Araldite block.

This work has demonstrated that it is very important to minimize the effects of stress on optical fibres with a core size of 50  $\mu\text{m}$ . The main source of stress in assemblies like the IFU is the slit block. The size of the block and the epoxy will have a strong influence on the FRD performance of the fibres.

## ACKNOWLEDGMENTS

This work was financially supported by the FAPESP project no. 1999/03744-1 and CNPq project 62.0053/01-1-PADCT III/Milenio. We wish to thank the staff of the Laboratório Nacional de Astrofísica/MCT and Instituto de Física de São Carlos/USP.

## REFERENCES

- Angel J. R. P., Adams M. T., Boroson T. A., Moore R. L., 1977, *ApJ*, 218, 776
- Barden S. C., Ramsey L. W., Truax R. J., 1980, *Bull. Am. Astron. Soc.*, 12, 460
- Barden S. C., Ramsey L. W., Truax R. J., 1981, *PASP*, 93, 154

- Carrasco E., Parry I. R., 1994, *MNRAS*, 271, 1
- Cesar A. C. et al., 2002, *Proc. SPIE* Vol. 4841, 1417
- Clayton C. A., 1989, *A&A*, 213, 502
- de Oliveira A. C. et al., 2003, in Masanori I., Moorwood A. F., eds, *Proc. SPIE* Vol. 4841, *Instrument Design and Performance for Optical/Infrared Ground-based Telescopes*. SPIE, Bellingham, p. 1417
- Gray P. M., 1983, in Boksenberg A., Crawford D. I., eds, *Proc. SPIE* Vol. 445, *Instrumentation in Astronomy V*, p. 57
- Guerin J., Felenbok P., 1988, in Barden C. S., ed., *ASP Conf. Ser. Vol. 3, Fiber Optics in Astronomy*. Astron. Soc. Pac., San Francisco, p. 52
- Kenworthy M. A., Parry I. R., Taylor K., 2001, *PASP*, 113, 215
- Lee D., Haynes R., Skeen D. J., 2001, *MNRAS*, 326, 774
- Lund G., Enard D., 1983, in Boksenberg A., Crawford D. I., eds, *Proc. SPIE* Vol. 445, *Instrumentation in Astronomy V*. SPIE, Bellingham, p. 65
- Murray G. et al., 2003, in Masanori I., Moorwood A. F., eds, *Proc. SPIE* Vol. 4841, *Instrument Design and Performance for Optical/Infrared Ground-based Telescopes*. SPIE, Bellingham, p. 1750
- Powell J. R., 1983, in Boksenberg A., Crawford D. I., eds, *Proc. SPIE* Vol. 445, *Instrumentation in Astronomy VI*. SPIE, Bellingham, p. 77
- Ramsey L. W., 1988, in Barden C. S., ed., *ASP Conf. Ser. Vol. 3, Fiber Optics in Astronomy*. Astron. Soc. Pac., San Francisco, p. 28
- Ramsey L. W., Huenemoerder D. L., 1986, in Crawford D. L., ed., *Proc. SPIE* Vol. 627, *Instrumentation in Astronomy VI*, p. 282
- Tody D., 1993, in Hanisch R. J., Brissenden R. J. V., Barnes J., eds, *ASP Conf. Ser. Vol. 52, Astronomical Data Analysis Software and Systems II*. Astron. Soc. Pac., San Francisco, p. 173

This paper has been typeset from a  $\text{\TeX/L\AA\TeX}$  file prepared by the author.